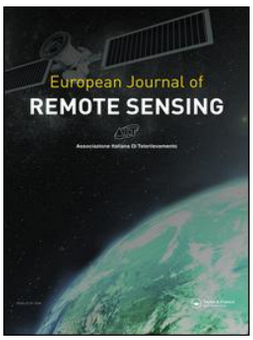

European Journal of Remote Sensing

ISSN: (Print) 2279-7254 (Online) Journal homepage: http://www.tandfonline.com/loi/tejr20

Seasonality of MODIS LST over Southern Italy and correlation with land cover, topography and solar radiation

Daniela Stroppiana, Massimo Antoninetti & Pietro Alessandro Brivio

To cite this article: Daniela Stroppiana, Massimo Antoninetti & Pietro Alessandro Brivio (2014) Seasonality of MODIS LST over Southern Italy and correlation with land cover, topography and solar radiation, European Journal of Remote Sensing, 47:1, 133-152

To link to this article: http://dx.doi.org/10.5721/EuJRS20144709

European Journal of Remote Sensing - 2014, 47: 133-152
doi: 10.5721/EuJRS20144709
Received 17/12/2012, accepted 16/08/2013

European Journal of Remote Sensing
An official journal of the Italian Society of Remote Sensing

www.aitjournal.com

Seasonality of MODIS LST over Southern Italy and correlation with land cover, topography and solar radiation

Daniela Stroppiana*, Massimo Antoninetti and Pietro Alessandro Brivio

Institute for the Electromagnetic Sensing of the Environment,
National Research Council (CNR-IREA), Via Bassini 15, 20133, Milano
*Corresponding author, e-mail address: stroppiana.d@irea.cnr.it

Abstract
Land Surface Temperature (LST) is a key variable in the interactions and energy fluxes between the Earth surface and the atmosphere. Satellite data provide consistent, continuous and spatially distributed information on the Earth's surface conditions among which LST. Ten years of NASA-MODIS day-time and night-time 1 km LST data over Southern Italy have been analyzed to quantify the influence of factors such as topography and the land cover on LST spatio-temporal variations. Results show that topography significantly influence LST variability as a function of the land cover and to a different extent for day-time and night-time data. Moreover, the relation between LST and the influential factors varies with the season during the year. This study contributes to a further understanding of the complex relationship between the spatio-temporal variability of the surface thermal conditions and its driving factors highlighting how these relationships might change within the year.

Keywords: MODIS, LST time series, land cover, topography, solar radiation, geothermal research.

Introduction
Land Surface Temperature (LST) is the radiation temperature measured at the interface between surface materials (top of plant canopy, water, ground, ice, or snow surface) and the atmosphere. It is a key parameter in the land surface radiation budget being an important variable in climate change studies [Brivio et al., 2001; Jin and Liang, 2006; Wan and Liang, 2009]. LST is also a factor controlling most physical, chemical and biological processes [Qin and Karnieli, 1999; Zhong et al., 2010] and, in particular, it is correlated to soil moisture and canopy evapotranspiration [Wan et al., 2004a; Wang and Liang, 2008].
Remote sensing techniques can provide information on the properties of the Earth from local to global scales with a high temporal frequency especially for surface characteristics that have a large spatial heterogeneity, such as LST [Wan and Liang, 2009]. Starting from the early missions, such as the Heat Capacity Mapping Missions (HCMM) carrying

the Heat Capacity Mapping Radiometer (HCMR) [Price, 1977; Watson et al., 1982; Cassinis et al., 1984; Vukovich, 1984], thermal infrared (TIR) data have been used to obtain information on the Earth surface temperature. Space-borne sensors carried by polar orbiting satellites with spectral bands in the TIR domain of the electromagnetic spectrum, allowed scientists to observe and monitor LST over large areas and long periods of time.

Data acquired by the NASA-MODIS (Moderate Resolution Imaging Spectroradiometer) sensor, beginning from the year 2000, significantly improve both geometric and radiometric characteristics of previous sensors, such as NOAA-AVHRR (National Oceanic and Atmospheric Administration-Advanced Very High Resolution Radiometer), besides being routinely processed to derive a suite of standard products for land/atmosphere/ocean monitoring [Justice et al., 2002; Tucker and Yager, 2011]. Among them, the MOD11A2 product provides estimates of LST and Emissivity (ε) from MODIS-Terra acquisitions at 10.30 am and 10.30 pm globally, at 1 km spatial resolution and every 8 days. MODIS LST data have been exploited in environmental studies such as monitoring urban heat island effect [Liu et al., 2007; Xiao et al., 2007; Retails et al., 2010; Keramitsoglou et al., 2011; Liu and Zhang, 2011], estimating air temperature [Huang et al., 2008; Son et al., 2012] and retrieving soil moisture mainly for agricultural applications [Benali et al., 2012]. Since LST is a key indicator of geothermal and geological activities below the Earth surface [Kahle et al., 1976; Cassinis et al., 1984] satellite data could also be exploited for geothermal exploration for searching alternative energy sources [Lee, 1978; Prakash et al., 1995; Fred et al., 2008; Qin et al., 2011]. Our work has developed in this research framework as preliminary analysis of the spatio-temporal variability of MODIS LST for investigating surface thermal anomalies at regional scale.

Spatio-temporal variability of LST at the regional scale is driven by influencing factors such as vegetation cover characteristics (fractional cover, canopy structure, vegetation surface roughness, albedo, leaf conductance), surface thermal properties (soil type and moisture), topography, incoming solar radiation and meteorological conditions [Julien et al., 2006; Van de Kerchove et al., 2013; Veraverbeke et al., 2013]. Moreover, many of these controlling parameters interact thus creating a very complex interpretation scheme [Sandholt et al., 2002]. The development of quantitative models that describe the relation between spatio-temporal variability of LST and the driving factor is therefore crucial [Van de Kerchove et al., 2013] although few studies have addressed this issue using remotely sensed data [Ge, 2010; Westermann et al., 2011; Van De Kerchove et al., 2013].

In this study we analyze day-time and night-time MODIS LST over Southern Italy as provided by the MOD11A2 product to investigate spatio-temporal variability of the surface temperature as a function of the land cover, topography (altitude) and potential solar radiation. According to previous studies, topography, land cover and incoming solar radiation and land cover are the major controlling factors on LST spatial distribution [Bertoldi et al., 2010]. Due to the relatively small size of the study area, latitudinal changes, which also influence surface temperatures, can be assumed negligible. The results presented in this paper are preliminary to further investigation of the presence of low enthalpy geothermal energy sources based on LST anomalies identified in the MODIS time series and cleaned of the most important influential factors analysed.

Study area and data

The study area

The study area covers a region of about 400 km * 400 km over Southern Italy (Fig. 1) and centered on the Basilicata, Campania, Molise and Puglia regions. The area is predominantly flat with 88% of the land area below 1000 m a.s.l. . Mountain areas run along the central part with the Apennines oriented from north-west to south-east. The highest regions are located at the southern end of the central Apennines range; lowlands cover a significant part of the study area with the major plain located in Northern Apulia (Tavoliere delle Puglie). According to the MODIS Land Cover Type (MCD12Q1) Collection 5 product (see section 2.3), more than 60% of the land area in the study region is agricultural land, followed by extensive urban areas (about 11%); forests cover approximately 10% of the study area.

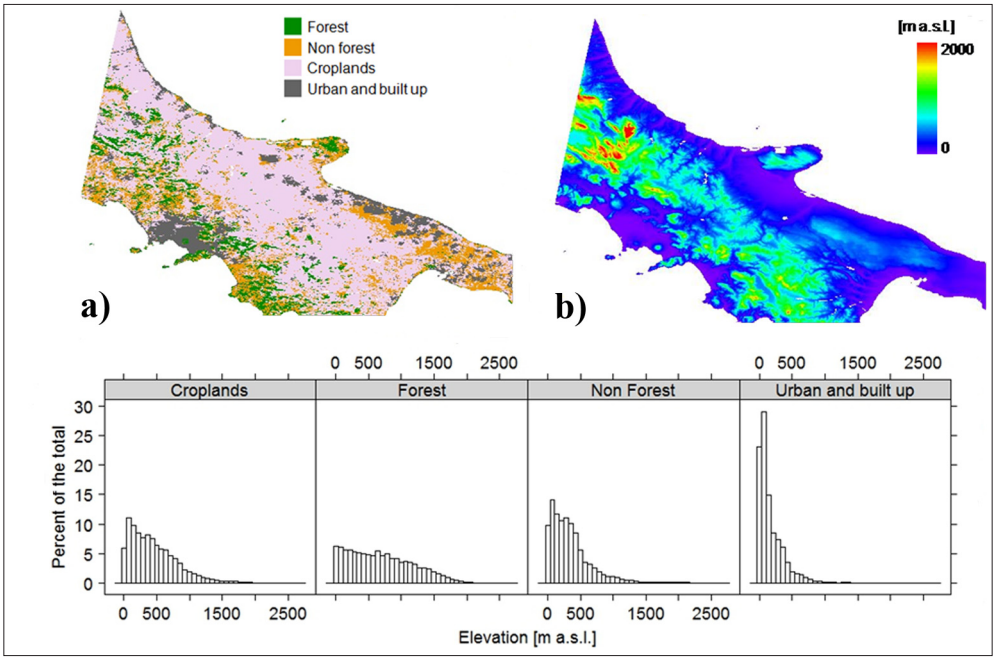

Figure 1 - (a) The land cover map as derived from the classification of the UMD land cover. (b) the Digital elevation Model (DEM) and at the bottom the histograms of frequency distribution of the elevation [m. a.s.l.] for the land cover classes.

The MOD11A2 product

The MOD11A2 Version-5 product (MODIS/Terra Land Surface Temperature/Emissivity 8-Day L3 Global 1km SIN Grid V005) provides 8 day composites of LST [K] at 1 km spatial resolution by averaging daily estimates [Wan et al., 2002]. This product includes estimates of day-time (10:30 am, Terra descending node) and night-time (10:30 pm, Terra ascending node) LST together with quality control layers which provide information on the accuracy of the retrievals (QC_day and QC_night). More details can be found in the

Collection-5 MODIS Land Surface Temperature Products Users' Guide (https://lpdaac.usgs.gov/products/modis_products_table, last access September 2013).
Ten years of the MOD11A2 product (2001-2010) have been downloaded from the USGS Glovis web site (http://glovis.usgs.gov/, last access September 2013) for tile h19 v04; LST and QC data provided as HDF (Hierarchical Data Format) files which have been subset over the study area, re-projected from Equal Area Sinusoidal projection to geographic Lat-Lon, WGS 84 coordinates.

The land cover map and the digital elevation model

In order to describe the distribution of the land cover in the study area, we chose the 1km UMD (University of Maryland) land cover map from the MODIS MCD12Q1 Collection 4 product [Friedl et al., 2010]. The original classes of the UMD map have been grouped into four major land covers: forest (UMD classes 1 to 5), non forest (UMD classes 6 to 10), croplands and urban areas; Table 1 shows the distribution of these classes in our study area. Although the spatial resolution of the UMD land cover is not optimal for the fragmented pattern of land covers in the study area, we preferred to maintain a resolution comparable to the LST dataset thus avoiding re-sampling. The aggregation into four large synthetic classes further reduces the influence of the coarse spatial resolution.
We also downloaded the Global Land One-km Base Elevation Digital Elevation Model (Globe DEM) [GLOBE Task Team, 1998] from the NOAA NESDIS web site (URL: http://www.ngdc.noaa.gov/mgg/topo/globe.html, last access September 2013). In this product elevation is provided globally for 1 km grid cells in geographic coordinate (Lat/Lon). Figure 1 shows the land cover map and the Globe DEM over the study area; at the bottom of the figure the histograms show the land cover type distribution as a function of elevation.

Table 1 - The distribution of the major and cover classes derived from the UMD (University of Maryland) land cover map and the percentage of the study area covered by each class.

Name	N pixels	Percent study area
Forest	6479	10%
Non forest	10509	17%
Croplands	39300	62%
Urban and built up	6934	11%

Methods

Table 2 summarizes the QC information provided with the MOD11A2 product. The so defined good quality data have an average error for emissivity ≤ 0.01 and for LST ≤ 1 K [Wan et al., 2004b]. If these accuracies for LST and emissivity estimates are not achieved, the pixel is classified with the other quality flag value and an estimation of the error is provided by bits 4 to 7 of the QC code (Tab. 2). We first analyzed the quality flags to investigate the proportion of missing and/or bad quality estimates within the ten-year dataset. Then, we computed LST monthly average and standard deviation over the period (2001-2010) to describe the seasonal behavior of LST and to quantify the year-by-year variability. All these analyses were carried out in the original MODIS sinusoidal projection.

Table 2 - The codes of the QC layer for the MOD11A2 product.

Bit N°	Name	Bit	Comment
0-1	Mandatory QA Flags	00	LST produced, good quality, not necessary to examine more detailed QA
		01	LST produced, other quality, recommend examination of more detailed QA
		10	LST not produced due to cloud effects
		11	LST not produced primarily due to reasons other than cloud
2-3	Data Quality Flag	00	Good data quality of L1B in 7 TIR bands
		01	Other quality data
		10	To be defined
		11	To be defined
4-5	Emis Error Flag	00	Average emissivity error<= 0.01
		01	Average emissivity error<= 0.02
		10	Average emissivity error<= 0.04
		11	Average emissivity error> 0.04
6-7	LST Error Flag	00	Average LST error <= 1K
		01	Average LST error <= 2K
		10	Average LST error <= 3K
		11	Average LST error > 3K

In the second part of our work we assessed the relationship between monthly average LST and topography (elevation), land cover and incoming solar radiation. MODIS data have been re-projected to geographic Lat/Lon coordinates and regression models were used to assess the influence of each variable on LST. Incoming solar radiation (or insolation) was computed with the Area Solar Radiation tool in the Solar Radiation Tools of ArcGIS 9.3 which computes the global incoming radiation across the landscape (image/raster) based on methods from the hemispherical view-shed algorithm [Rich, 1990; Rich et al., 1994; Fu and Rich, 2002]. The output raster map provides monthly solar radiation (Watt Hour m-2) with the same spatial resolution of the input DEM (in our case, 1 km) and the same projection (Lat/Lon). The tool computes the potential solar radiation from the sun position as a function of the day and time of the year and takes into account only the latitude range, variations in elevation, orientation (slope and aspect) and shadows cast by topographic features from the input DEM.

Results and discussion

LST time series: quality and gap issues

Figures 2 and 3 show example 2001-2010 time series of day- and night-time MODIS LST (black line) and QC (colored dots) for pixels over cropland, non forest and forest land cover classes of the study area. The gaps in the LST time series are those satellite observations that are discarded due the presence of clouds (red dots).

The frequency of the quality flags over the entire dataset is reported in Table 3 for day- and night-time LST. Both datasets have a high rate of good quality data (>60%) mainly because compositing over 8-day periods reduces the proportion of gaps produced by daily missing observations. In the night-time dataset there is a greater proportion of good quality LST estimates (QC=0 and QC=17) and a larger proportion of pixels flagged as cloudy (3%), which are probably due to false detections in night-time images since reflectance bands are not available for accurate cloud

detection [Wan and Liang, 2009]. Among the pixels assigned the other quality flag value, the most frequent class is of pixels with average error in LST estimation less than 2K (QC=65) and it covers 25% and 28% of the night- and day-time data, respectively.

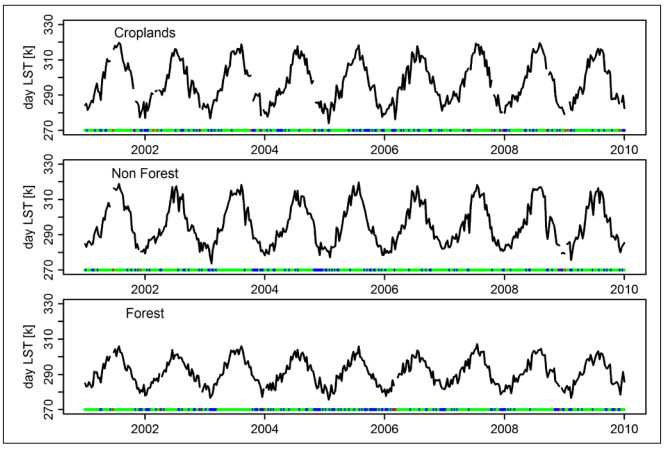

Figure 2 - Time series of the day-time MODIS Land Surface Temperature (LST) for the period 2001-2010 (black line) with quality information (green: good data, red: cloudy, yellow: average error emissivity <= 0.02, blue: average error emissivity <= 0.01 & average error LST <= 2K, cyan: average error emissivity<=0.02 & average error LST <= 2K) for example pixels from the croplands, non forest and forest classes.

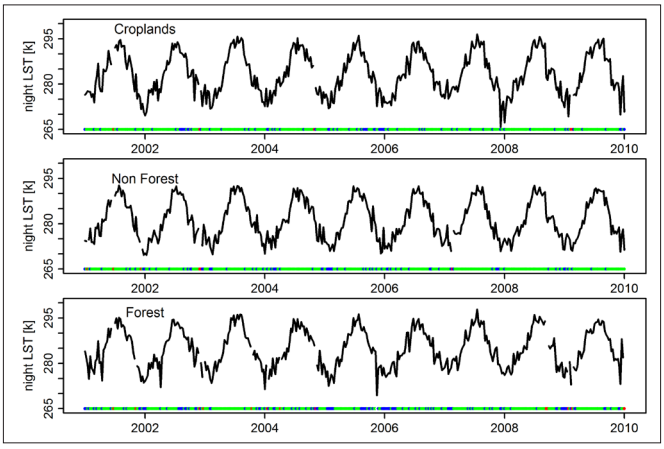

Figure 3 - Time series of the night-time MODIS Land Surface Temperature (LST) for the period 2001-2010 (black line) with quality information (green: good data, red: cloudy, yellow: average error emissivity <= 0.02, blue: average error emissivity <= 0.01 & average error LST <= 2K, cyan: average error emissivity<=0.02 & average error LST <= 2K) for example pixels from the croplands, non forest and forest classes.

Table 3 - The frequency of the quality flags as observed in the 2001-2010 day and night MODIS LST time series over the study area. Flag values that were not covered by at least 1% of the pixels were discarded. QC = Quality control, LST = Land Surface Temperature.

QC value (0-255)	Description	Day LST	Night LST
0	Good quality	60.57%	63.16%
2	LST not computed due to the presence of clouds	2.67%	3.01%
17	LST produced, average emissivity error <=0.02 & average LST error <= 1K	1.05%	1.99%
65	LST produced, average emissivity error <=0.01 & average LST error <= 2K	28.31%	25.43%
81	LST produced, average emissivity error <=0.02 & average LST error <= 2K	6.60%	5.86%

Figure 4 shows the percentage of good quality day- and night-time LST estimates over land for each 8-day period of the year. The proportion of good data increases from the lowest values in winter (highest percentage of cloudy pixels) to the greatest in summer (predominant clear sky conditions). In July and August (periods 24 to 31 on the x-axis), more than 80% of the land pixels in the study area are assigned the good quality class, meaning that LST is retrieved with the highest accuracy. The graph also shows that there are very few outliers (circle markers) thus suggesting a consistent accuracy in the multi-year datasets. These figures confirm that the proportion of good quality data is consistent between the two datasets; neither the day- or the night-time LST is retrieved with a significantly higher accuracy over the ten years analyzed.

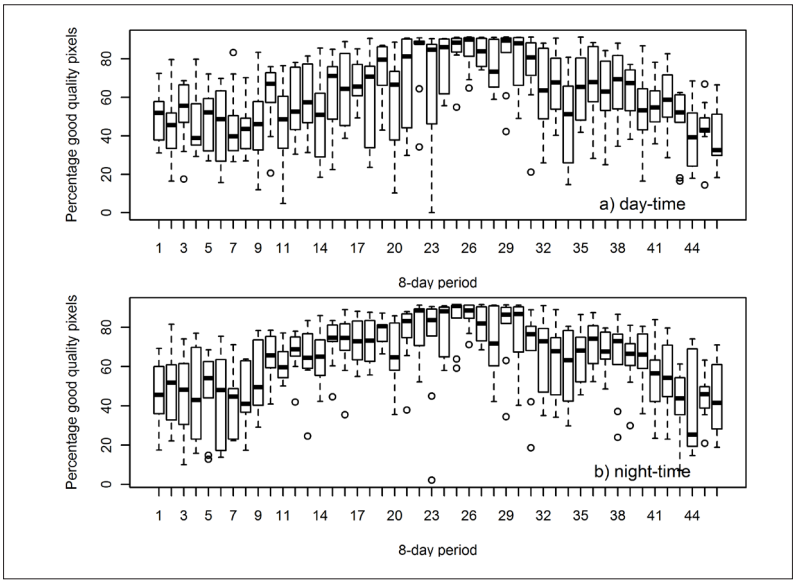

Figure 4 - Box-plot of the percentage of good quality day- and night-time LST from the MODIS Quality Control (QC) layer computed for each 8-day period. Median, upper and lower quartiles, and outliers are represented by the thick black line, the upper and lower boundary of the rectangle and the empty circle markers, respectively. All graphs are produced in RStudio, Version 0.97.551.

Figure 5 shows the proportion of pixels flagged as other quality (lower accuracy) of day-time (top row) and night-time LST (bottom row) for the four land cover classes of Table 1. The quality of LST retrievals over vegetated pixels show the same trend as the entire dataset (Fig. 4) with the lowest proportion of good quality data in winter. The urban and built up class is assigned poorer quality flags throughout the year; although a seasonal behavior can be observed, the proportion of lower quality pixels is greater than 70%. These results suggest that MODIS LST estimates over urban areas might be less reliable compared to other land cover classes. In general LSTs are higher and more variable than concurrent air temperatures due to the complexity of the surface types (i.e., industrial areas, commercial areas, airports, and residential areas), in urban environments and variations in urban topography [Keramitsoglou et al, 2011].
For our purposes (regression and correlation analysis) we deemed the accuracy of LST estimates provided by the MOD11A2 dataset sufficient. Since gaps in the time series cover a small proportion (<3%) of the data, we deemed not necessary to apply interpolation procedures. Moreover, our study focuses on the analysis of LST variability which implies the use of average values which reduces the influence of local missing data.

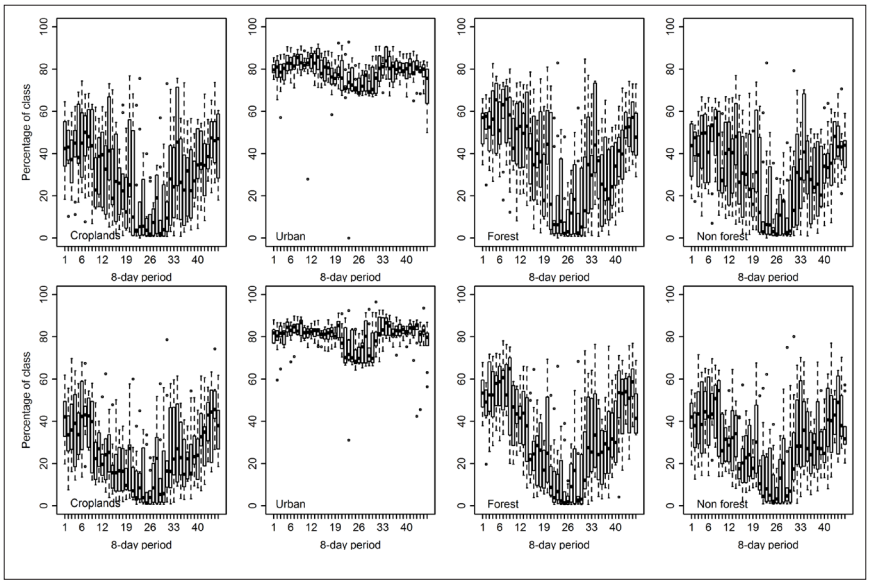

Figure 5 - Box-plot of the percentage of other quality day- (top row) and night-time (bottom row) LST from the MODIS Quality Control (QC) layer computed for each 8-day period for the four land cover classes. Median, upper and lower quartiles, and outliers are represented by the thick black line, the upper and lower boundary of the rectangle and the empty circle markers, respectively. All graphs are produced in RStudio, Version 0.97.551.

Monthly LST

Figure 6 shows average monthly day-time LST and standard deviation as derived from the 2001-2010 dataset. LST increases from the winter lowest values to the highest values in summer. The spatial variability of LST reflects the topography of the region as shown by the DEM of Figure 1. Indeed, higher elevation regions are characterized by average monthly LST lower than the lowlands and this difference is greater during the summer

months (June to August) when, for example, the plain area of the Apulia region is warmer than the higher regions along the Apennines. Moreover, mountain areas are characterized by extreme variability of topography (steep slopes and altitude variations) which could also determine a significant variability of LST [Bertoldi et al., 2010]; Figure 6 shows in fact a greater spatial variability of LST along the Apennines chain. For what concerns the inter-annual variability of LST, as observed in the standard deviation values, most of the pixels fall in the range 1-4 K (blue, green and yellow regions). Some notable exceptions are February and March when greater standard deviations (stdev > 4.0 K) are probably due to the effect of different times of snow melting from one year to the other. Higher standard deviation values in months such as August and October could be due to residual clouds over mountain areas. The flat areas along the Adriatic and Tyrrhenian coasts are characterized by the lowest variability as shown by the blue regions of the standard deviation maps thus suggesting that the year to year variability of MODIS LST is lower than in mountain areas.

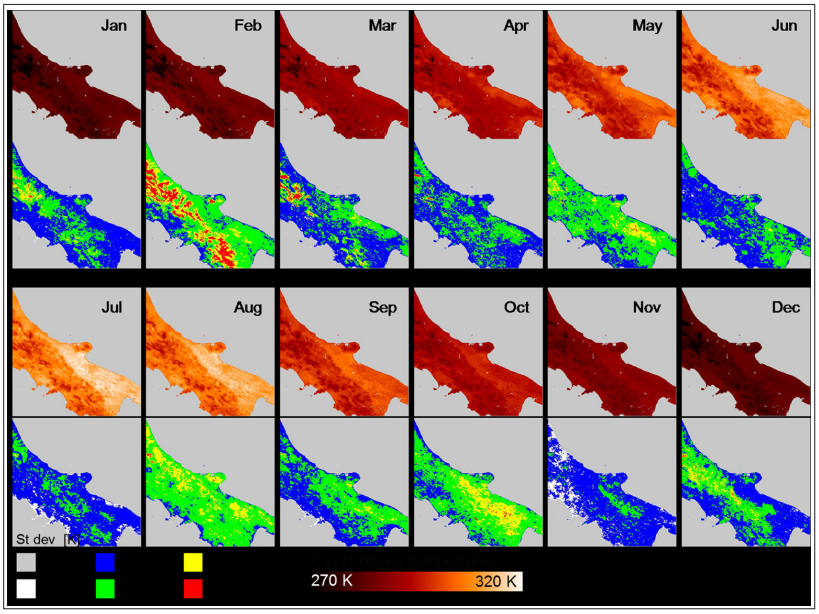

Figure 6 - Average monthly day-time Land Surface Temperature (LST) [K] (first and third rows) and standard deviation [K] (second and fourth rows) as derived from the 2001-2010 multiyear dataset.

LST and elevation

Figures 7 and 8 show the linear regression models between average monthly day-time and night-time LST and elevation. Table 4 present the coefficient of determination R^2 for the four land cover classes. The negative Pearson-r (Figs. 7 and 8) confirms the well-known relationship between surface temperature and topography. In fact, LST decreases with increasing elevation [Hais and Kučera, 2009] for two major reasons: air temperature decreases with elevation and vegetation tends to be vertically organized [Bertoldi et al., 2010]. Our results highlight a significant difference in this relationship between the day- and night-time LST. First, the range of values

for Pearson-r is narrower for night-time data compared to day-time: 0.74-0.90 and 0.69-0.92, respectively. Second, the correlation between day-time LST and elevation is greater in winter months (December to February) and lower in summer (July-August) for all land cover classes; the opposite is observed for night-time LST. Other authors pointed out the greater correlation between night-time LST and elevation with respect to day-time LST [Fu and Rich, 2002; Pouteau et al., 2011; Van De Kerchove et al., 2013], but our results add that this relation is not consistent throughout the year.

The scatter plots also show the effect of the vegetation altitudinal distribution on day-time LST; starting in spring and with a maximum in July and August, points are more scattered around the regression line for lower regions where the variety of the land cover types is greater compared to higher areas (see histograms in Fig. 1). Vegetation characteristics play a primary role on how incoming solar radiation, which during the day is the direct source of energy, affects LST [Geiger et al., 2003]. The different effects of incoming radiation on the land cover types are mainly related to their stature and structure which influence turbulent heat transfer, radiation divergence and transpiration [Korner et al., 2003; Wohlfahrt et al., 2003; Bertoldi et al., 2010], hence LST. The absence of solar radiation at night annul the role of vegetation; indeed, the points of LST are homogeneously scattered along the regression line for all months of the year (Fig. 8).

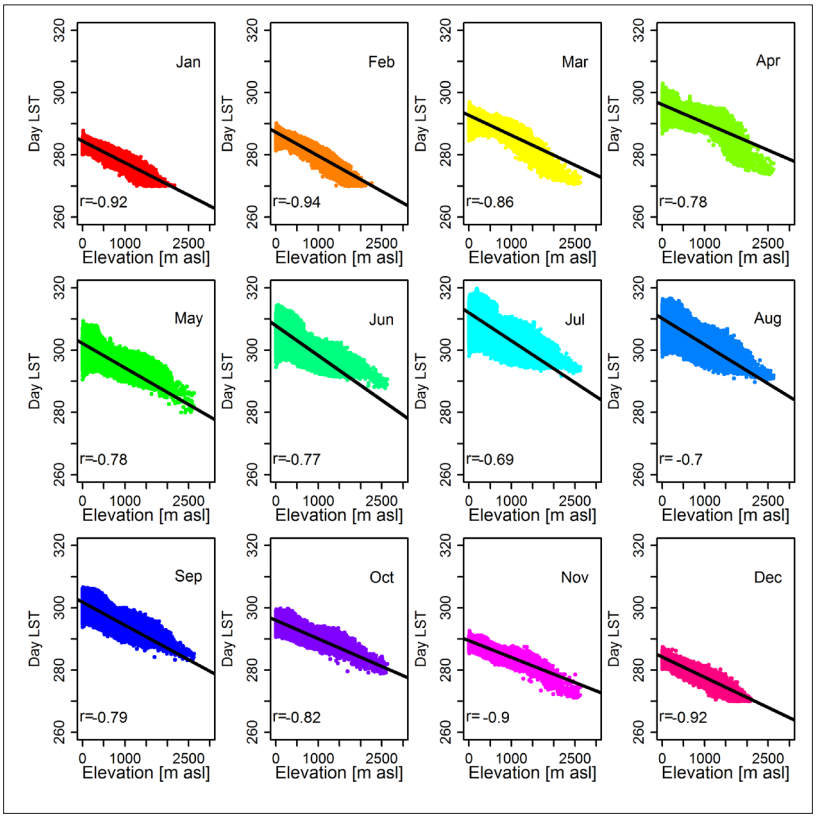

Figure 7 - Linear regression models showing the relationship between average monthly day-time Land Surface temperature (LST) and elevation [m. a.s.l.].

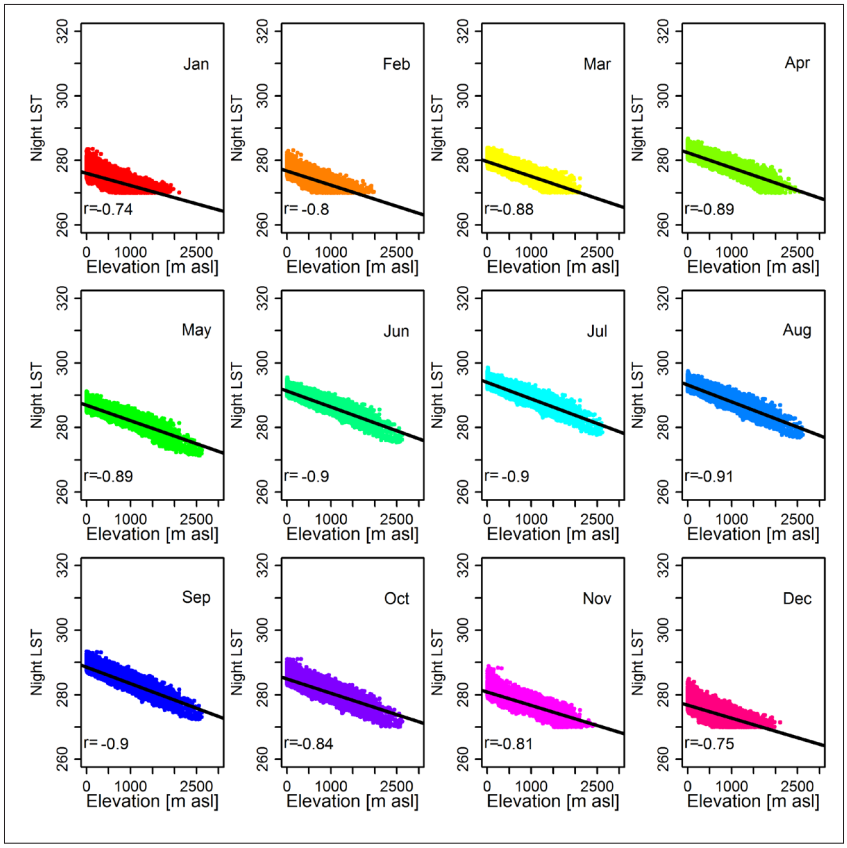

Figure 8 - Linear regression models showing the relationship between average monthly night-time Land Surface temperature (LST) and elevation [m. a.s.l.].

Table 4 - The coefficient of determination R^2 showing the correlation between average monthly day- and night-time LST and elevation for the land cover classes of the study area.

R^2	LST	J	F	M	A	M	J	J	A	S	O	N	D
Forest	Day	.88	.90	.74	.64	.67	.67	.58	.66	.79	.83	.86	.86
	Night	.64	.71	.79	.81	.79	.81	.79	.81	.81	.76	.72	.67
Non forest	Day	.79	.83	.67	.53	.43	.40	.32	.38	.59	.67	.79	.79
	Night	.55	.61	.72	.79	.79	.81	.79	.83	.83	.74	.66	.55
Crops	Day	.83	.88	.74	.62	.64	.62	.50	.49	.59	.62	.77	.85
	Night	.58	.67	.81	.83	.85	.85	.83	.86	.86	.77	.72	.62
Urban	Day	.61	.62	.30	.26	.24	.21	.12	.14	.32	.41	.58	.66
	Night	.37	.49	.59	.61	.62	.64	.59	.66	.64	.52	.46	.40

The difference between the day-time and night-time regression models varies with the class (Tab. 4): the difference is lowest (greatest) for the forest (urban) classes. In urban areas, the relation between night-time LST and elevation observed in summer months is significantly greater than the relation with day-time LST, with R^2 dropping below 0.3. The fact that in urban areas the correlation between LST and elevation is

lower during the day means that other factors influence LST variability, such as for example, solar radiation.

LST and land cover

Figure 9 shows 2001-2010 average monthly day- and night-time LST and LST day-night difference as boxplot graphs. The color keys represent the four land cover classes: forest, non forest, croplands and urban as red, green, cyan and purple, respectively. Day- and night-time LST show a clear seasonality through the months with a peak in July when the median values (black thick line) of day LST are above 300 K for the vegetated classes and almost 310 K for the urban class. Night-time maxima also occur in July but with median class values in the range 290-295 K.

All of the four land cover classes show an increase in the variability of day-time LST (inter-quartile range, the colored rectangle) from winter months up to the maxima in the June to August period. The largest increase of variability is observed for the non forest and croplands classes probably due to a larger heterogeneity of the vegetation characteristics within the class. Each 1 km pixel could in fact be composed by different land covers with different proportions (fragmented landscape). Moreover, LST is related to the physiological activities of leaves over fully vegetated areas (forests) and to a combination of both soil and canopy temperatures over sparse vegetation [Van Leeuwen et al., 2011]; it is likely that soil moisture has a greater variability thus leading to a larger range of LST values over sparser non forested areas. The same within class variability is not observed for night-time data; LST at day-time hours has been shown to have a greater heterogeneity compared to night-time LST because of the effect of solar radiation [Kahle et al., 1976]. Day-time heterogeneity has indeed a clear seasonal variation due to the surface incident solar radiation, the land cover and soil moisture.

Most of the outliers (black circle markers) are negatively biased towards the lowest values with a greater proportion of them in night-time data; these extremely low values could be due to undetected clouds which are more frequent in the night-time dataset when the visible bands are not available for accurate cloud masking . Thin clouds (e.g. cirrus) cloud detection is difficult and the pixel might pass the test and be identified as clear sky [Ackerman et al., 1998]. Cloud contamination remains a major issue in processing optical/thermal satellite data for land monitoring since clouds prevent from observing the Earth surface. The use of temporal composites rather than daily products, such as in the case of the MOD11A2 product, reduces the influence of cloud contamination although it does not solve it. Moreover, the least proportion of outliers in day-time surface temperature occurs in summer months when clear sky conditions are prevalent.

LST difference shows also an increase during the year with maximum values above 15 K for the non forest, croplands and urban classes. The forest class has the lowest difference between day and night temperatures due to the cooling effect of forests [Van Leeuwen et al., 2011]; denser vegetation canopies prevent incoming radiation from reaching the surface and increasing the temperature; this effect also combines with a greater amount of evapotranspiration of dense canopies which has a cooling effect [Van Leeuwen et al., 2011]. Other authors reported that non forested areas experience a

greater cooling effect at night than forested regions [Goulden et al., 2006; Van Leeuwen et al., 2011; Van De Kerchove et al., 2013] with greater surface temperatures when vegetation gets denser.

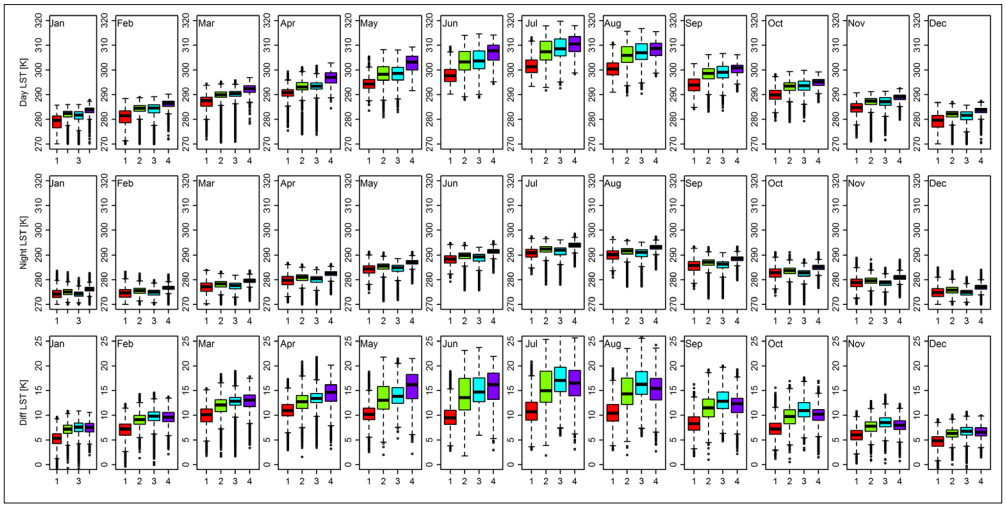

Figure 9 - Average monthly day- and night-time LST [K] and day-night difference for the land cover classes (1=forest, 2=non forest, 3=croplands, 4=urban and built up). Median, upper and lower quartiles, and outliers are represented by the thick black line, the upper and lower boundary of the rectangle and the empty circle markers, respectively. All graphs are produced in RStudio, Version 0.97.551.

Finally, the day-night difference shows the greatest values for cropland areas which have a high surface temperature during the day which decreases significantly during the night; this effect can be observed when compared to the non forest class. The urban areas have the highest surface temperatures in both day- and night-time datasets in all months because of the urban heat island effect (UHI) [Schwarz et al., 2011] and the greatest day-night difference with the exception of the June to September period.

LST and solar radiation

Figures 10 and 11 show the scatter plots of average monthly day- and night-time LST vs. potential solar radiation for altitude classes and figure 12 presents the histograms of the R^2 coefficient of determination for each land cover class and all classes together. As shown by scatter plots and the histograms, correlation is very low for day-time surface temperature if altitude is not taken into account and it increases in summer months when incoming radiation is greater. When the land cover is taken into account, forested areas show the greatest correlation; in non forest and croplands regions day surface temperature is not correlated to solar radiation probably because other factors affect LST spatio-temporal variability. As observed before this classes might be very heterogeneous and all factors interact to determine LST variability. Correlation significantly increases for nigh-time surface temperature with the highest values in summer months.

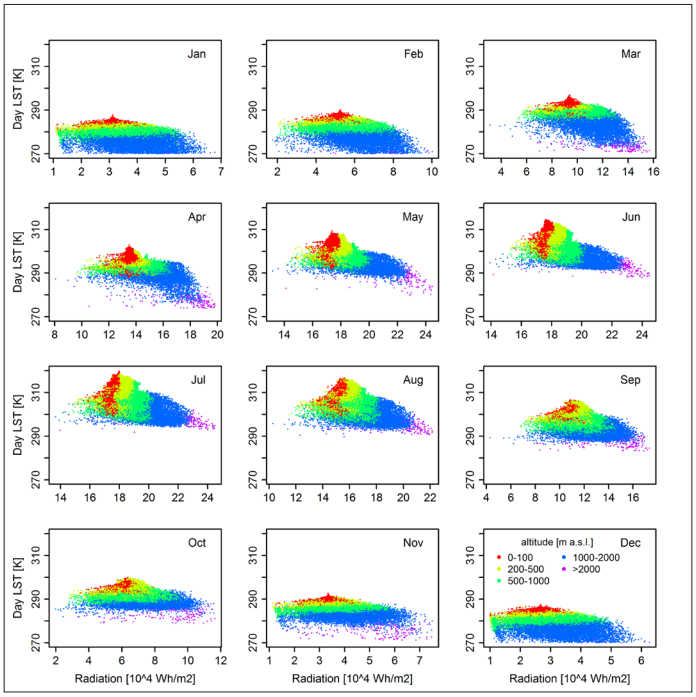

Figure 10 - Scatter plots of monthly day-time LST vs. potential radiation for altitude classes.

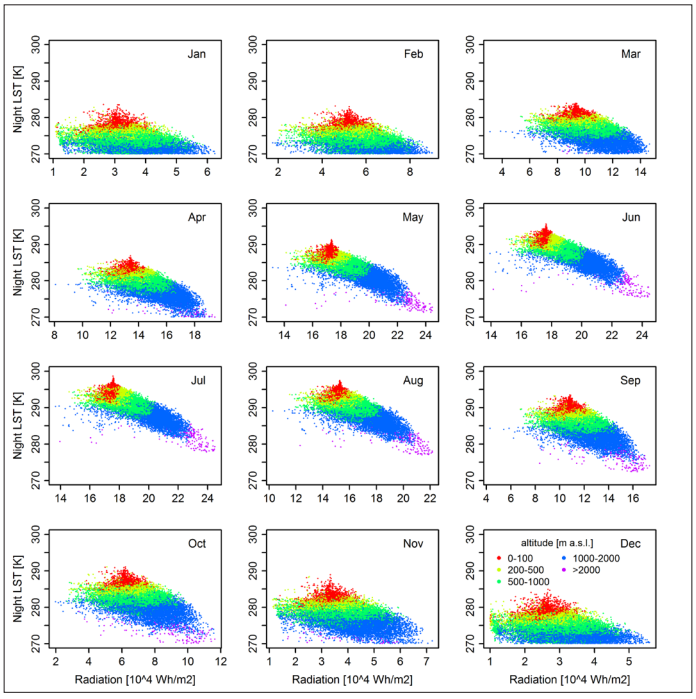

Figure 11 - Scatter plots of monthly night-time LST vs. potential radiation for altitude classes.

Other authors found no clear relationship between surface temperature time series and solar radiation [Daly et al., 2008; Pouteau et al., 2011; Van De Kerchove et al., 2013] suggesting that topography and insolation play an important role on the local scale climatology rather than on regional processes.

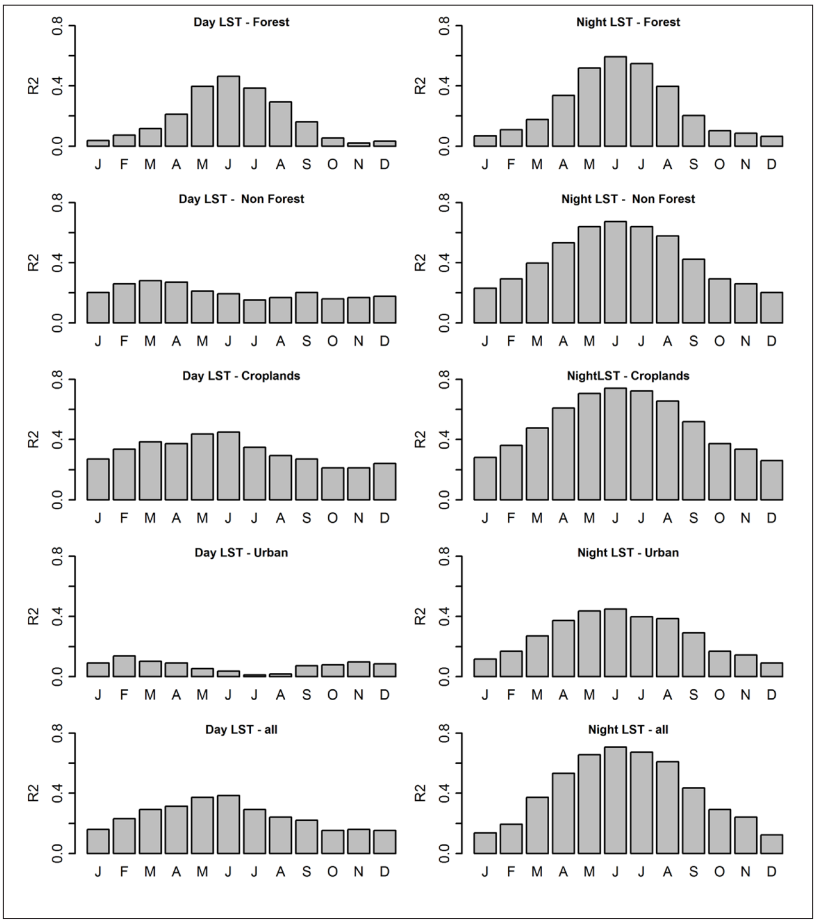

Figure 12 - Histograms of the coefficient of correlation R^2 between LST day and night and solar radiation for the land cover classes and for all data together.

Conclusions and future activities

We analysed ten years (2001-2010) of MODIS day-time and night-time 8-day LST at 1 km resolution over Southern Italy to characterize the spatial and temporal variability of the surface temperature and its variability with topography, land cover and potential solar radiation. These regional analyses are preliminary for the investigation of thermal anomalies of the Earth surface temperature in the framework of the characterization of geothermal sources. We first analysed the quality flags provided with the MOD11A2 product and found that the quality varies during the year mainly as a function of the cloud cover (winter/ summer seasons). We did not observe a significant difference between day-time and night-

time quality but our analyses highlighted that urban areas have a significant proportion of data with very poor quality flags (low accuracy of LST estimates).
The regression analysis showed that monthly LST is significantly correlated to topography (altitude) although correlation varies with the month of the year and with the land cover. We highlighted that in summer months the correlation with topography significantly decreases due to vegetation development at lower altitudes which play a role in the energy fluxes exchange between the surface and the atmosphere. The spatio-temporal variations of LST are indeed influenced by the land cover characteristics which in particular influences the thermal excursion between day and night surface temperatures. Finally, we observed in our dataset that incoming solar radiation, which should be the direct factor to influence surface temperature, is not significantly correlated to LST if the contribution of other factors (e.g. altitude and land cover) cannot be separated. Our analyses confirm the high spatio-temporal variability of LST and, compared to previous work, show that the correlation with factors such as topography and the land cover changes with the season (summer/winter). Despite the coarse resolution, MODIS LST data can be used for rapid identification of surface temperature anomalies at the regional scale to be further investigated with local measurements.

Acknowledgements

This work has been carried out within the research project “Atlante Geotermico” funded by the MEF (Italian Ministry of Economy and Finance) and coordinated by National Research Council of Italy (CNR).

References

Ackerman S., Strabala K., Menzel P., Frey R., Moeller C., Gumley L. (1998) - *Discriminating clear sky from clouds with MODIS*. Journal of Geophysical Research, 103: 141-157. doi: http://dx.doi.org/10.1029/1998JD200032.

Benali A., Carvalho A.C., Nunes J.P., Carvalhais N., Santos A. (2012) - *Estimating air surface temperature in Portugal using MODIS LST data*. Remote Sensing of Environment, 124: 108-121. doi: http://dx.doi.org/10.1016/j.rse.2012.04.024.

Bertoldi G., Notarnicola C., Leitinger G., Endrizzi S., Zebisch M., Della Chiesa S., Tappeneir U. (2010) - *Topographical and ecohydrological controls on land surface temperature in an alpine catchment*. Ecohydrology, 3 (2): 189-204.

Brivio P.A., Colombo R., Meroni M. (2001) - *The use of remotely sensed data for the estimation of energy balance components in a mountainous catchment*. In: Remote Sensing and Climate Modelling: Synergies and Limitations, M. Beniston & M. Verstraete (Eds.), Kluwer Academic Publishers, Dordrecht/The Netherlands, pp. 307-327. doi: http://dx.doi.org/10.1007/0-306-48149-9_13.

Cassinis R., Tosi N., Lechi G.M., Brivio P.A., Zilioli E., Marini A. (1984) - *Thermal inertia of rocks: An HCMM experiment on Sardinia, Italy*. International Journal of Remote Sensing, 5 (1): 79-94. doi: http://dx.doi.org/10.1080/01431168408948790.

Daly C., Halbleib M., Smith J.I., Gibson W.P., Doggett M.K., Taylor G.H., Curtis J., Pasteris P.P. (2008) - *Physiographically sensitive mapping of climatological temperature and precipitation across the conterminous United States.* International Journal of Climatology, 28 (15): 2031-2064. doi: http://dx.doi.org/10.1002/joc.1688.

Fred G.R., Watson R.E., Lockwood W.B., Newman T.N., Anderson R.A.G. (2008) - *Development and comparison of Landsat radiometric and snowpack model inversion techniques for estimating geothermal heat flux*. Remote Sensing of Environment, 112 (2): 471-481. doi: http://dx.doi.org/10.1016/j.rse.2007.05.010.

Friedl M.A., Sulla-Menashe D., Tan B., Schneider A., Ramankutty N., Sibley A., Huanga X. (2010) - *MODIS Collection 5 global land cover: Algorithm refinements and characterization of new datasets*. Remote Sensing of Environment, 114 (1): 168-182. doi: http://dx.doi.org/10.1016/j.rse.2009.08.016.

Fu P., Rich P.M. (2002) - *A geometric solar radiation model and its applications in agriculture and forestry.* Computers and Electronics in Agriculture, 37 (1-3): 25-35. doi: http://dx.doi.org/10.1016/S0168-1699(02)00115-1.

Ge J. (2010) - *MODIS observed impacts of intensive agriculture on surface temperature in the southern Great Plains*. International Journal of Climatology, 30: 1994-2003. doi: http://dx.doi.org/10.1002/joc.2093.

Geiger R., Aron R.H., Todhunter P. (2003) - *The Climate Near the Ground*. Rowman and Littlefield Publishers, (6th Ed.) Lanham, MD.

GLOBE Task Team and others (Hastings David A., P. K. Dunbar, G. M. Elphingstone, M. Bootz, H. Murakami, Peter Holland, Nevin A. Bryant, Thomas L. Logan, J.-P. Muller, Gunter Schreier and John S. MacDonald, Eds. (1998) - *The Global Land One-kilometer Base Elevation (GLOBE) Digital Elevation Model, Version 1.0*. National Oceanic and Atmospheric Administration, National Geophysical Data Center, 325 Broadway, Boulder, Colorado 80303, USA. Digital Database on the World Wide Web World Wide Web and CD-ROMs.

Goulden M.L., Miller S.D., da Rocha H.R. (2006) - *Nocturnal cold air drainage and pooling in a tropical forest*. Journal of Geophysical research, 111 (D8), D08S04. doi: http://dx.doi.org/10.1029/2005JD006037.

Hais M., Kučera T. (2009) - *The influence of topography on the forest surface temperature retrieved from Landsat TM, ETM + and ASTER thermal channels.* ISPRS Journal of Photogrammetry and Remote Sensing, 64 (6): 585-591. doi: http://dx.doi.org/10.1016/j.isprsjprs.2009.04.003.

Huang C., Li X., Lu L. (2008) - *Retrieving soil temperature profile by assimilating MODIS LST products with ensemble Kalman filter*. Remote Sensing of Environment, 112 (4): 1320-1336. doi: http://dx.doi.org/10.1016/j.rse.2007.03.028.

Jin M., Liang S. (2006) - *Improving land surface emissivity parameter of land surface models in GCM.* Journal of Climate, 19: 2867-2881. doi: http://dx.doi.org/10.1175/JCLI3720.1.

Julien Y., Sobrino J.A., Verhoef W. (2006) - *Changes in land surface temperatures and NDVI values over Europe between 1982 and 1999*. Remote Sensing of Environment 103 (1): 43-55. doi: http://dx.doi.org/10.1016/j.rse.2006.03.011.

Justice C.O., Townshend J.R.G., Vermote E.F., Masuoka E., Wolfe R.E., Saleous N., Roy D.P., Morisette J.T. (2002) - *An overview of MODIS land data processing and product status*. Remote Sensing of Environment, 83: 3-15. doi: http://dx.doi.org/10.1016/S0034-4257(02)00084-6.

Kahle A.B., Gillespie A.R., Goetz A.F.H. (1976) - *Thermal inertia imaging: a new geologic mapping tool*. Geophysical Research Letters, 3: 26-28. doi: http://dx.doi.org/10.1029/GL003i001p00026.

Keramitsoglou I., Chris T., Kiranoudis C.T., Ceriola G., Weng Q., Rajasekar U. (2011) - *Identification and analysis of urban surface temperature patterns in Greater Athens, Greece, using MODIS imagery*. Remote Sensing of Environment, 115 (12): 3080-3090. doi: http://dx.doi.org/10.1016/j.rse.2011.06.014.

Korner C., Paulsen J., Pelaz-Riedl S. (2003) - *A bioclimatic characterization of Europe's alpine areas.* In: Alpine Biodiversity in Europe, Ecological Studies, Nagy L, Grabherr G, Korner C, Tompson D. (Eds). Springer, Berlin, 167: 13-28. doi: http://dx.doi.org/10.1007/978-3-642-18967-8_2.

Lee K. (1978) - *Analysis of thermal infrared imagery of the Black Rock Desert geothermal area.* Colorado School of Mines Quarterly, 4 (2): 31-44.

Liu L., Zhang Y. (2011) - *Urban Heat Island Analysis Using the Landsat TM Data and ASTER Data: A Case Study in Hong Kong*. Remote Sensing of Environment, 3 (7): 1535-1552. doi: http://dx.doi.org/10.3390/rs3071535.

Liu Y., Yamaguchi Y., Ke C. (2007) - *Reducing the discrepancy between ASTER and MODIS Land Surface Temperature products*. Sensors, 7: 3043-3057. doi: http://dx.doi.org/10.3390/s7123043.

Prakash A., Sastry R.G.S., Gupta R.P., Saraf A.K. (1995) - *Estimating the depth of buried hot features from thermal IR remote sensing data: a conceptual approach*. International Journal of Remote Sensing, 16 (13): 2503-2510. doi: http://dx.doi.org/10.1080/01431169508954572.

Price J.C. (1977) - *Thermal Inertia Mapping: A New View of the Earth*. Journal of Geophysical Research, 82 (18): 2582-2590. doi: http://dx.doi.org/10.1029/JC082i018p02582.

Pouteau R., Rambal S., Ratte J.P., Gogé F., Joffre R., Winkel T. (2011) - *Downscaling MODIS-derived maps using GIS and boosted regression trees; the case of frost occurrence over the Andean highlands of Bolivia*. Remote Sensing of Environment, 115: 117-129. doi: http://dx.doi.org/10.1016/j.rse.2010.08.011.

Qin Q., Zhang N., Nan P., Chai L. (2011) - *Geothermal area detection using Landsat ETM+ thermal infrared data and its mechanistic analysis - A case study in Tengchong, China*. International Journal of Applied Earth Observation, 13: 552-559. doi: http://dx.doi.org/10.1016/j.jag.2011.02.005.

Qin Z., Karnieli A. (1999) - *Progress in the remote sensing of land surface temperature and ground emissivity using NOAA-AVHRR data*. International Journal of Remote Sensing, 20: 2367-2393. doi: http://dx.doi.org/10.1080/014311699212074.

Retails A., Paronis D., Lagouvardos K., Kotron V. (2010) - *The heat wave of June 2007 in Athens, Greece-Part 1 : Study of satellite derived land surface temperature*. Atmospheric Research, 98 (2-4): 458-467. doi: http://dx.doi.org/10.1016/j.atmosres.2010.08.005.

Rich P.M. (1990) - *Characterizing plant canopies with hemispherical photography*. Remote Sensing Reviews, 5: 13-29. doi: http://dx.doi.org/10.1080/02757259009532119.

Rich P.M., Hetrickw A., Savings C., Dubayah R. (1994) - *Viewshed analysis for calculation of incident solar radiation: applications in ecology*. Proceedings of the ASPRS-ACSM Convention (Bethesda, MD: ASPRS), pp. 524-529.

Sandholt I., Rasmussen K., Andersen J. (2002) - *A simple interpretation of the surface temperature/vegetation index space for assessment of surface moisture status*. Remote Sensing of Environment, 79 (2-3): 213-224. doi: http://dx.doi.org/10.1016/S0034-4257(01)00274-7.

Son N.T., Chen C.F., Chen C.R., Chang L.Y., Minh V.Q. (2012) - *Monitoring agricultural drought in the Lower Mekong Basin using MODIS NDVI and land surface temperature data*. International Journal of Applied Earth Observation, 18: 417-427. doi: http://dx.doi.org/10.1016/j.jag.2012.03.014.

Schwatz N., Lautenbach S., Seppelt R. (2011) - *Exploring indicators for quantifying surface urban heat islands of European cities with MODIS land surface temperatures*. Remote Sensing of Environment, 115 (12): 3175-3186. doi: http://dx.doi.org/10.1016/j.rse.2011.07.003.

Tucker C.J., Yager K.A. (2011) - *Ten Years of MODIS in space: lessons learned and future perspectives*. European Journal of Remote Sensing, 43: 7-18. doi: http://dx.doi.org/10.5721/ItJRS20114331.

Van de Kerchove R., Lhermitte S., Veraverbeke S., Goossens R. (2013) - *Spatio-temporal variability in remotely sensed land surface temperature, and its relationship with physiograhic variables in the Russian Altay Mountains*. International Journal of Applied Earth Observation, 20: 4-19. doi: http://dx.doi.org/10.1016/j.jag.2011.09.007.

Van Leeuwen T.T., Frank A.J., Jin Y., Smuth P., Goulden M.L., vand der Werf G.R., Randerson J.T. (2011) - *Optimal use of land surface temperature data to detect changes in tropical forest cover.* Journal of Geophysical Research, 116 (G02002). doi: http://dx.doi.org/10.1029/2010JG001488.

Veraverbeke S., Verstraeten W.W., Lhermitte S., Van De Kerchove R., Goossens R. (2013) - *Assessment of post-fire changes in land surface temperature and surface albedo, and their relation with fire–burn severity using multitemporal MODIS imagery.* International Journal of Wildland Fire, 21 (3): 243-256. doi: http://dx.doi.org/10.1071/WF10075.

Vukovich F.M. (1984) - *A comparison of surface temperature derived from HCMM infrared measurements with field data*. Remote Sensing of Environment, 15: 63-76. doi: http://dx.doi.org/10.1016/0034-4257(84)90052-X.

Wan K., Liang S. (2009) - *Evaluation of ASTER and MODIS land surface temperature and emissivity products using long-term surface longwave radiation observations at SURFRAD sites*. Remote Sensing of Environment, 113: 1556-1565. doi: http://dx.doi.org/10.1016/j.rse.2009.03.009.

Wan Z., Zhang Y., Zhang Q., Li Z. (2002) - *Validation of the land-surface temperature products retrieved from Terra Moderate Resolution Imaging Spectroradiometer data*. Remote Sensing of Environment, 83:163-180. doi: http://dx.doi.org/10.1016/S0034-4257(02)00093-7.

Wan Z., Wang P., Li X. (2004a) - *Using MODIS land surface temperature and normalized difference vegetation index products for monitoring drought in the Southern Great Plains, USA*. International Journal of Remote Sensing, 25 (1): 61-72. doi: http://dx.doi.org/10.1080/0143116031000115328.

Wan Z., Zhang Y., Zhang Q., Li Z.L. (2004b) - *Quality assessment and validation of the MODIS global land surface temperature*. International Journal of Remote Sensing, 25: 261-274. doi: http://dx.doi.org/10.1080/01431160310001164l7.

Wang K., Liang S. (2008) - *An improved method for estimating global evapotranspiration based on satellite determination of surface net radiation, vegetation index, temperature, and soil moisture*. Journal of Hydrometeoroly, 9 (4): 712-727. doi: http://dx.doi.org/10.1175/2007JHM911.1.

Watson K., Hummermiller S., Sawatzky D.L. (1982) - *Registration of Heat-Capacity Mapping Mission day and night images*. Photogrammetric Engineering & Remote Sensing, 48 (2): 263-268.

Westermann S., Langer M., Boike J. (2011) - *Spatial and temporal variations of summer surface temperatures of high-arctic tundra on Svalbard - Implications for MODIS LST based permafrost monitoring*. Remote Sensing of Environment, 115 (3): 908-922. doi: http://dx.doi.org/10.1016/j.rse.2010.11.018.

Wohlfahrt G., Bahn M., Newesely CH., Sapinsky S., Tappeiner U., Cernusca A. (2003) - *Canopy structure versus physiology effects on net photosysnthesis of mountain grasslands differing in land use*. Ecological Modelling, 170: 407-426. doi: http://dx.doi.org/10.1016/S0304-3800(03)00242-4.

Xiao R., Ouyang Z., Heng H., Li W., Schienke E., Wang X. (2007) - *Spatial pattern of impervious surfaces and their impacts on land surface temperature in Beijing, China*. Journal of Environmental Sciences, 19: 250-256. doi: http://dx.doi.org/10.1016/S1001-0742(07)60041-2.

Zhong L., Ma Y., Su Z., Salama M.S. (2010) - *Estimation of Land Surface Temperature over the Tibetan Plateau Using AVHRR and MODIS data*. Advances in Atmospheric Sciences, 27 (5): 1110-1118. doi: http://dx.doi.org/10.1007/s00376-009-9133-0.